

Influence of the Third Dimension of Quasi-Two-Dimensional Cuprate Superconductors on Angle-Resolved Photoemission Spectra

A. Bansil¹, M. Lindroos^{1,2}, S. Sahrakorpi¹, and R.S. Markiewicz¹

¹*Physics Department, Northeastern University, Boston, Massachusetts 02115, USA*

²*Institute of Physics, Tampere University of Technology, P.O. Box 692, 33101 Tampere, Finland*
(Dated: November 20, 2018)

Angle-resolved photoemission spectroscopy (ARPES) presents significant simplifications in analyzing strictly two-dimensional (2D) materials, but even the most anisotropic physical systems display some residual three-dimensionality. Here we demonstrate how this third dimension manifests itself in ARPES spectra of quasi-2D materials by considering the example of the cuprate $\text{Bi}_2\text{Sr}_2\text{CaCu}_2\text{O}_8$ (Bi2212). The intercell, interlayer hopping, which is responsible for k_z -dispersion of the bands, is found to induce an irreducible broadening to the ARPES lineshapes with a characteristic dependence on the in-plane momentum k_{\parallel} . Our study suggests that ARPES lineshapes can provide a direct spectroscopic window for establishing the existence of coherent c -axis conductivity in a material via the detection of this new broadening mechanism, and bears on the understanding of 2D to 3D crossover and pseudogap and stripe physics in novel materials through ARPES experiments.

PACS numbers: 79.60.-i, 71.18.+y, 74.72.Hs

Angle-resolved photoemission spectroscopy (ARPES) has been applied extensively in the recent years for investigating the electronic and quasiparticle properties of high-temperature superconductors¹. Much of the existing ARPES work on the cuprates and other quasi-2D materials implicitly assumes perfect two-dimensionality, ignoring the effects of dispersion in the third dimension. As energy resolutions of the order of a few meV's have now become possible in the state-of-the-art ARPES instrumentation, it is natural to ask the question: How will k_z -dispersion play out in the ARPES spectra of the quasi-2D materials? An obvious answer is that spectral peaks will undergo shifts with photon energy –albeit small– much like in the 3D case.^{3,4,5} Our analysis however reveals a very different scenario in that insofar as ARPES response to k_z -dispersion is concerned, quasi-2D systems differ fundamentally from their 3D counterparts. We find that in the presence of typical final state dampings of the order of eV's, initial state dispersions over much smaller energy scales will not appear as energy shifts with $\hbar\nu$, but will instead induce an irreducible linewidth in the spectral peaks with a characteristic k_{\parallel} dependence.

Our results bear on a variety of important issues in cuprate physics and give insight into a number of puzzling features of ARPES in the cuprates. Since our new broadening mechanism does not have its origin in a scattering process, it explains why the lifetimes derived from ARPES spectra are generally found to be shorter than those obtained from other experiments. Moreover, Fermi surface (FS) maps obtained via ARPES often display broad patches of spectral weight rather than well-defined FS imprints, particularly near the antinodal point; such patches occur naturally in our calculations. Indeed, much of the *pseudogap* phenomena – in particular the lack of well-defined quasiparticles near $(\pi, 0)$ – will need to be reevaluated in light of the present findings. In this vein, these results also impact the analysis of stripe physics through ARPES experiments. Finally, detection of the k_z

related linewidths in the ARPES spectra offers a unique spectroscopic window for establishing the existence of coherent c -axis conductivity and intercell coupling in a system; this important intrinsic property is not accessible directly through other techniques.¹

Specifically, we focus in this article on the tetragonal body-centered $\text{Bi}_2\text{Sr}_2\text{CaCu}_2\text{O}_8$ (Bi2212) compound, which has been a workhorse of ARPES studies. Bi2212 is a nearly 2D material with two CuO_2 -layers in the primitive unit cell. The *intracell* interaction between the two CuO_2 -layers, spaced a relatively short distance of ~ 3.2 Å apart, results in the well-known bilayer splitting^{1,6,7,8,9,10}. On the other hand, the *intercell* coupling between the bilayer slabs in different unit cells is expected to be smaller due to the larger intercell Cu-Cu distance of ~ 12 Å resulting in weak but *non-vanishing* k_z -dispersion. The intercell coupling will be even more pronounced in other high-Tc's since Bi2212 presents one of the longest c -axes in the cuprate family.

Concerning computational details, the band structure for Bi2212 was obtained within the local-density-approximation (LDA) by using the well-established Green's function methodology¹¹. The crystal potential used is the same as that employed in our previous studies of Bi2212 and involves 30 atoms per conventional unit cell^{6,7,12}, yielding good agreement with the experimentally observed Fermi surface (FS)^{10,13,14,15,16}. ARPES intensities have been computed within the one-step photoemission formalism; see, Refs. 6 and 7 for details.

Figure 1(a), which considers the familiar antibonding (A) and bonding (B) bands in Bi2212, shows that the k_{\parallel} -dispersion depends strongly on k_z as the associated bands wander over the two sets of shaded areas. The k_z -dispersion (i.e. the vertical width of the shaded areas) displays a striking dependence on k_{\parallel} and nearly vanishes at the antinodal point $k_{\parallel} = (\pi/a, 0)$. A clear bilayer splitting between the A and B bands is seen at all k -values, except at $k_{\parallel} = k_{\parallel}^* = 0.2(2\pi/a)$ for $k_z = 0$ (solid

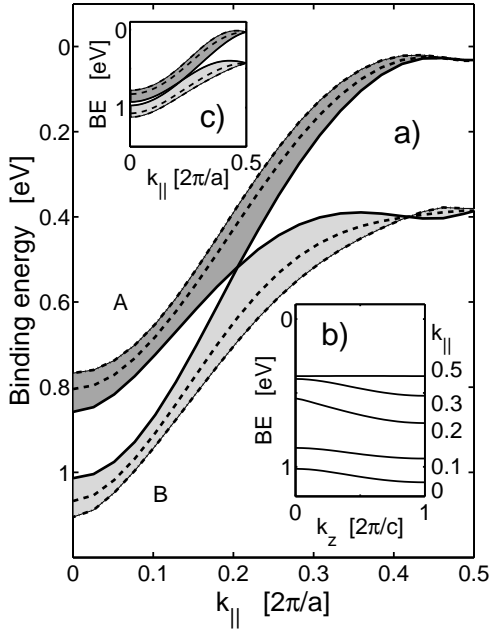


FIG. 1: (a): Calculated first-principles k_{\parallel} -dispersion in Bi2212 along [100]-direction for the B and A bands at three different k_z values (in units of $2\pi/c$): $k_z = 0$ (solid lines); $k_z = 0.5$ (dashed), and $k_z = 1$ (dash-dotted). Shading denotes the regions over which the bands wander as a function of k_z . (b): k_z -dispersion of the B band at five different k_{\parallel} values ranging from 0 to π/a . (c): Same as (a), except that these results are based on a tight binding formalism.

lines), where A and B bands touch. This level crossing leads to the anomalous k_z -dispersion shown in Fig. 1(b) for the B band: The shape changes from being described approximately by the form $\sin^2(k_z c/4)$ for $k_{\parallel} = 0$, to $|\sin(k_z c/4)|$ at k_{\parallel}^* , and finally back to $\sin^2(k_z c/4)$ for $k_{\parallel} a/(2\pi) = 0.5$. The antibonding band behaves similarly (not shown for brevity). The complex behavior of the bilayer splitting and the k_z -dispersion shown in the first-principles computations of Figs. 1(a) and 1(b) can be modeled reasonably well by a relatively simple tight-binding (TB) Hamiltonian as seen from Fig. 1(c). We return below to discuss this point further.

We next turn our attention to how k_z -dispersion will manifest itself in ARPES spectra. The key insight in this regard is provided by the simulations¹⁷ of Fig. 2, which consider the evolution of the lineshape of the energy distribution curves (EDCs) as the final state broadening introduced via the imaginary part of the final state self-energy¹⁸, Σ_f'' , is increased from a very small value in (a) to a realistic value in (c). In (a), the position of the spectral peak undergoes the familiar shift as $h\nu$ varies. This shift results from the fact that in the photoexcitation process k_{\parallel} must remain unchanged in transmission of the electron across the surface and the initial and final states can connect only at a specific value of k_z in order to conserve energy. Note that the total shift in the peak position in the EDCs of (a) gives the size of

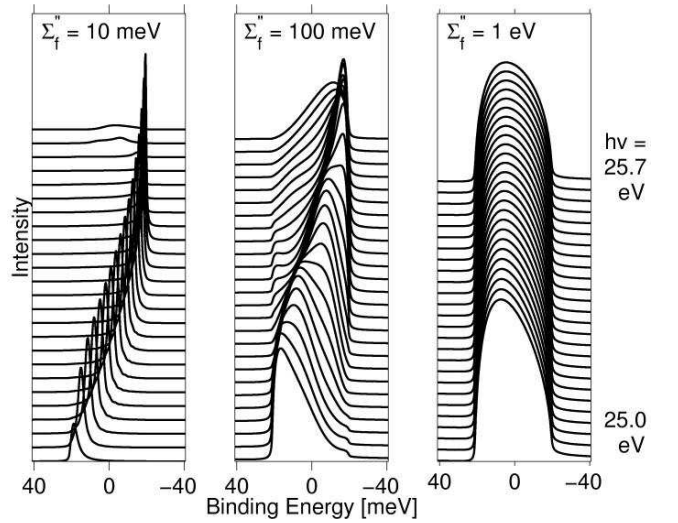


FIG. 2: Simulated ARPES lineshapes (EDCs) in Bi2212 for a series of photon energies ($h\nu = 25 - 25.7$ eV) at a fixed $k_{\parallel} = (0.34, 0.09)2\pi/a$ -point using three different values of the final state broadening given by the indicated imaginary parts of the self-energy, Σ_f'' . In order to highlight the influence of k_z -dispersion, the initial state broadening is chosen to be very small, $\Sigma_i'' = 0.2$ meV.¹⁷

the k_z -dispersion of the initial state. This should not be confused with the change in $h\nu$ needed to probe such a band. The change in $h\nu$ is controlled by the final state dispersion, which is generally much larger than that of the initial state.

Continuing to the intermediate case of $\Sigma_f'' = 0.1$ eV in Fig. 2(b), the shift in the peak position from the bottom to the top of the initial state band is once again evident, but the lineshapes are quite different, even though the initial state damping Σ_i'' in (b) is identical to that in (a). It is striking that some spectral intensity appears in (b) at all energies encompassed by the initial state band at every $h\nu$. This remarkable effect comes about because the energy uncertainty permitted by the width of the final state allows the photoelectron to couple with initial states off-the-energy-shell. The lineshape thus develops a new component with an $h\nu$ -independent width equal to the initial state bandwidth, which rides on top of the energy conserving peak in (a). Notice also how the changes in the peak position could allow observing different FSs as one maps different values of k_z . Finally, for the realistic final state width of $\Sigma_f'' = 1$ eV in (c), the initial state bandwidth component dominates the lineshape. The lineshape of the EDC curve is now virtually $h\nu$ -independent. Despite the large final-state broadening, the energy spread of the EDC remains equal to the *initial state bandwidth in k_z -direction* because outside of this interval, there are no initial state electrons capable of absorbing the photon.

Fig. 3 elaborates on these points by considering some of the results of Fig. 2 over a much broader range of photon energies. Fig. 3(a) presents the spectra of Fig. 2(b)

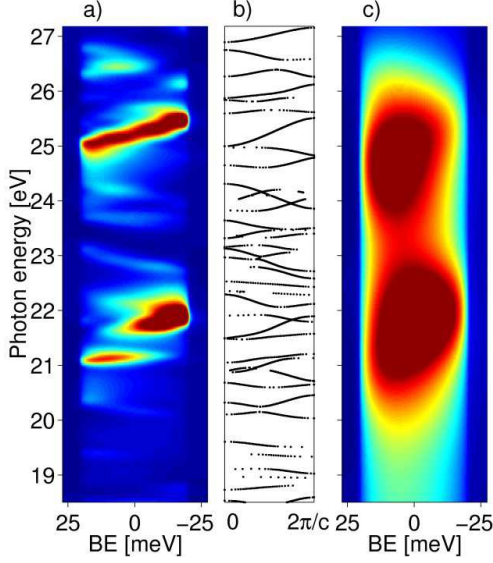


FIG. 3: (Color) (a) Simulated ARPES intensities of Fig. 2(b) are depicted over a wide photon energy range of 19 – 27 eV for $\Sigma_f'' = 0.1$ eV. Reds denote highs. (b) Final state band structure as a function of k_z . (c) Same as (a) except that $\Sigma_f'' = 1$ eV, which corresponds to the case of Fig. 2(c).

for $\Sigma_f'' = 0.1$ eV for $h\nu \approx 19 - 27$ eV. Different colored bands here represent the same initial states being excited to different final states. Comparing Figs. 3(a) and 3(b), we see that the peaks of Fig. 3(a) more or less follow the final state band structure of Fig. 3(b) [The agreement is not expected to be perfect of course, since the initial state dispersion is not entirely negligible]. In Fig. 3(c), when a more realistic final state width of $\Sigma_f'' = 1$ eV is assumed, much of the structure is lost. The large variations in colors (or intensities) observed in Figs. 3(a) and 3(c) are the consequence of the well-known k_{\parallel} and $h\nu$ -dependency of the ARPES matrix element.^{1,6,7,15,19}

The preceding discussion of Figs. 2 and 3 makes it obvious that in a quasi-2D system, k_z -dispersion leads to an irreducible linewidth in the ARPES spectra, which cannot be resolved by changing photon frequency. This effect will also appear in the FS maps observed by measuring emission from E_F in the (k_x, k_y) -plane. Fig. 4 illustrates how this plays out. The standard bilayer split FS in the $k_z = 0$ plane, given in Fig. 4(a), is the FS usually thought to be measured in ARPES. In Fig. 4(b) the full 3D FS has been projected on to the (001)-plane by collecting individual FS cuts corresponding to different k_z values. The k_z -dispersion is now seen to introduce an effective "broadening" to the FS imprint. In a perfect 2D-system, the maps in (b) and (a) would be identical. The effect of using a finite energy window of ± 30 meV around E_F in the computations is shown in Figs. 4(c) and 4(d). These simulations indicate the influence of a finite experimental resolution on the results.^{13,20} Note that even with the window of ± 30 meV in (d), the broadening effect of k_z -dispersion is not washed out. In fact, the broadening is

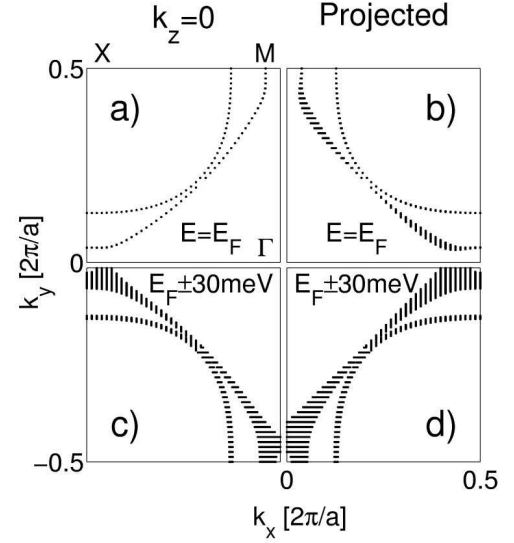


FIG. 4: Different imprints of the FS of Bi2212. (a): Section of the FS at $k_z = 0$. (b): Projection of the FS on to the (001)-plane, where the "broadening" of the FS reflects the effect of k_z -dispersion. (c) and (d) correspond to (a) and (b), respectively, except that the effect of adding a finite energy window of ± 30 meV is included in the computations.

somewhat enhanced, especially near the antinodal point due to the contribution of the flat bands related to the van Hove singularity (VHS).

It is also interesting to consider changes in the linewidth in momentum, Δk , as one moves away from the Fermi level. In general, our simulations indicate that Δk increases with increasing binding energy (BE), due mainly to the flattening of bands and the concomitant reduction in the band velocity.⁴ In any event, the broadening as a function of BE is neither simply quadratic nor exponential. Furthermore, considering the effect of varying Σ_i'' at a general k_{\parallel} -point, we have found that as the initial state damping due to intrinsic scattering mechanisms (simulated via the value of Σ_i'') decreases, the linewidth ΔE becomes increasingly dominated by the irreducible width associated with k_z -dispersion. Along the antinodal direction this dispersion is negligible, and ΔE and Σ_i'' are related linearly.²¹

We return now to comment briefly on the bands of Figs. 1(a) and 1(b). Insight into how the complex k_{\parallel} - and k_z -dependencies of these bands reflect *intercell* as well as *intracell* hopping effects can be gained by modeling these bands within the TB framework. In the absence of intercell coupling, the conventional bilayer splitting possesses the form $t_{bi} = t_z(c_x - c_y)^2$, with $c_i = \cos(k_i a)$, $i = x, y$. The *intercell* coupling in the cuprates may be included in the one-band model with dispersion²² $\epsilon_k = -2t(c_x + c_y) - 4t'c_x c_y - T_z(k_{\parallel}, s_z)[(c_x - c_y)^2/4 + a_0]$, where $s_z = \sin(k_z c/4)$ and $a_0 = 0.6$ corrects for the finite bilayer splitting found at $k_{\parallel} = 0$. The form of T_z depends on the particular cuprate considered. While Ref. 22 lists seven inequivalent interlayer hopping

parameters, we find that we can describe the dispersion reasonably by including only the dominant contribution associated with hopping between Cu 4s levels by introducing $T_z = \pm \sqrt{(t_z - t'_z)^2 + 4t_z t'_z s_z^2}$, where plus (minus) sign refers to the bonding (antibonding) solution. t_z is a constant associated with intracell interlayer hoppings, and $t'_z = 4t'_{z0} \cos(k_x a/2) \cos(k_y a/2)$ accounts for intercell hopping. The extra angular dependence in this term arises because for intercell hopping the two CuO₂-planes are offset, so that one Cu atom sits above an empty cell. Note that for $t'_z = 0$ one obtains the simple bilayer splitting t_{bi} with no k_z -dispersion. TB bands of Fig. 1(c) assume (in eV): $t = 0.42$, $t' = -0.12$, $t_z = 0.125$, and $t'_{z0} = 0.04$. A comparison of the first principles and TB bands in Figs. 1(a) and 1(c), respectively, shows that our TB model reproduces the bilayer splitting, the collapse of the k_z -dispersion around $(\pi/a, 0)$, and the anomalous dispersions associated with level crossing to a reasonably good degree, some minor discrepancies notwithstanding.

We emphasize that t'_z , which provides intercell coupling, is essential for obtaining coherent c -axis conductivity. t'_z thus controls the intrinsic resistivity anisotropy and gives a measure for discriminating between coherent and incoherent c -axis hopping.²³ The lifetimes in the cuprates extracted from ARPES are considerably smaller than optical lifetimes or those deduced from transport or tunneling measurements²⁴. A part of this difference may be explained to be the result of an unresolved bilayer splitting²⁵. The remaining anomalous broadening is often interpreted²⁶ in terms of small-angle scattering, which does not contribute to transport, but its origin remains obscure²⁷. The present analysis indicates that part of the broadening of ARPES lines has its origin in the k_z -dispersion, unrelated to any scattering mechanism.

Our predicted effects of k_z -dispersion on the linewidths in Bi2212 should be resolvable with the power of currently available high resolution ARPES instrumentation.²⁸ The size of our novel line broadening

mechanism will be larger in materials with greater 3D character (e.g. YBCO, LSCO, NCCO, ruthenates, manganites, etc.), although we expect the results of Figs. 1-4 to provide at least a qualitative handle in quasi-2D materials more generally. Notably, coherent 3D coupling has recently been reported in a Tl cuprate²⁹. Additionally, a similar k_z -induced broadening may be expected to have an impact on other experimental probes, such as Raman scattering³⁰.

In conclusion, we have demonstrated that residual k_z -dispersion in quasi-2D materials will induce an *irreducible linewidth* in ARPES spectra. This intrinsic linewidth offers a new spectroscopic window for understanding in- as well as out-of-plane scattering mechanisms and the nature of the 2D to 3D crossover in the cuprates. This highly anisotropic line broadening mechanism, which has not been recognized previously and is unrelated to 2D physics, indicates that the existing analysis of stripe and pseudogap physics based on ARPES spectra should be reexamined. Our study shows how ARPES can be extended to unravel the hidden third dimension of energy bands and Fermi surfaces in quasi-2D systems with wide-ranging consequences for understanding the nature of electronic states in many novel materials.

Acknowledgments

This work is supported by the US Department of Energy contract DE-AC03-76SF00098, and benefited from the allocation of supercomputer time at NERSC, Northeastern University's Advanced Scientific Computation Center (ASCC), and the Institute of Advanced Computing (IAC), Tampere. One of us (S.S.) acknowledges Suomen Akatemia and Vilho, Yrjö ja Kalle Väisälän Rahasto for financial support.

¹ A. Damascelli et al., Rev. Mod. Phys. 75, 473 (2003).

² Throughout this article, z -axis is defined to be normal to the Cu-O planes.

³ J.E. Inglesfield and E.W. Plummer on S.D. Kevan (ed.), *Angle Resolved Photoemission, Theory and Current Applications*, Elsevier 1992.

⁴ N.V. Smith et al., Phys. Rev. B 47, 15476 (1993).

⁵ M. Lindroos et al., Phys. Rev. Lett. 77, 2985 (1996).

⁶ A. Bansil et al., Phys. Rev. Lett. 83, 5154 (1999).

⁷ M. Lindroos et al., Phys. Rev. B 65, 054514 (2002).

⁸ D.L. Feng et al., Phys. Rev. Lett. 86, 5550 (2001).

⁹ Y.-D. Chuang et al., Phys. Rev. Lett. 87, 117002 (2001).

¹⁰ P. V. Bogdanov et al., Phys. Rev. B 64, 180505(R) (2001).

¹¹ See, e.g., A. Bansil et al., Phys. Rev. B 60, 13396 (1999), and references therein.

¹² The well-known "Bi pockets" in the vicinity of the M -point have been lifted above the Fermi energy by modifying the Bi and O potentials, consistent with experimental data.

¹³ It should be kept in mind that LDA calculations systematically overestimate band dispersions, typically by a factor of about 2-4.

¹⁴ A. Bansil et al., J. Phys. Chem. Solids 63, 2175 (2002).

¹⁵ M. C. Asensio et al., Phys. Rev. B 67, 014519 (2003).

¹⁶ Y.-D. Chuang et al., Phys. Rev. B 69, 094515 (2004).

¹⁷ The spectra have not been convoluted with the Fermi function throughout this article.

¹⁸ The imaginary part of the self-energy Σ'' is proportional to the inverse of the lifetime of the (quasi)particle in that state.

¹⁹ S. Sahrakorpi et al., Phys. Rev. B 68, 054522 (2003).

²⁰ The ± 30 meV window used would simulate an effective experimental resolution of about ± 8 meV [see Ref. 13].

²¹ The situation at the nodal point is more complicated, due to a small residual bilayer splitting. See also A.A. Kordyuk et al., cond-mat/0311137 (unpublished).

²² O.K. Andersen et al., J. Phys. Chem. Solids 56, 1573

- (1995).
- ²³ Of course, in Bi2212, the anomalous temperature dependence of ρ_c strongly hints that it is incoherent.
- ²⁴ B.W. Hoogenboom et al., Phys. Rev. B **67**, 224502 (2003).
- ²⁵ P.V. Bogdanov et al., Phys. Rev. Lett. **89**, 167002 (2002)
- ²⁶ E. Abrahams et al., Proc. Natl. Acad. Sci. **97**, 5714 (2000).
- ²⁷ A.J. Millis et al., Phys. Rev. B **67**, 214517 (2003).
- ²⁸ Note from Fig. 1 that a typical broadening is a significant fraction of the full bilayer splitting, which is experimentally found to be about 100 meV [recall Ref. 13].
- ²⁹ N.E. Hussey et al., Nature **425**, 814 (2003).
- ³⁰ T.P. Devereaux et al., Phys. Rev. B **59**, 6411 (1999).